Chinese Chemical Letters 35 (2024) 108556

Contents lists available at ScienceDirect

Chinese Chemical Letters

journal homepage: www.elsevier.com/locate/cclet

Polysaccharide based supramolecular injectable hydrogels for *in situ* treatment of bladder cancer☆

Chang Zhang[a], Jie Niu[a], Jianqiu Li[a], Hui Zhang[a], Qilin Yu[b,*], Yong Chen[a,*], Yu Liu[a,*]

[a] College of Chemistry, State Key Laboratory of Elemento-Organic Chemistry, Nankai University, Tianjin 300071, China
[b] College of Life Sciences, Key Laboratory of Molecular Microbiology and Technology, Nankai University, Tianjin 300071, China

ARTICLE INFO

Article history:
Received 27 March 2023
Revised 1 May 2023
Accepted 9 May 2023
Available online 10 May 2023

Keywords:
Sulfobutylether-β-cyclodextrin
Supramolecular chemistry
Chitosan
Injectable hydrogel
Bladder cancer
Local chemotherapy

ABSTRACT

Implantable system maximizes drug concentration and continuously releases drugs near the tumor, which is an effective tool to solve the difficult retention of chemotherapy drugs in bladder cancer. In this work, a novel polysaccharide supramolecular injectable hydrogel (CCA hydrogels for short) is rapidly constructed by simply mixing cationic chitosan, anionic sulfobutyl ether β-cyclodextrin (SBE-β-CD) and a trace amount of silver ions. The injected hydrogel reconstituted and regained its shape in less than 1 h, and it can still maintain the elasticity suitable for the human body. By packaging the drug directly, the gel achieves a high concentration of doxorubicin, an anticancer drug. Using MB49-luc cells as the model of bladder tumor for anti-tumor *in vivo*, the CCA-DOX gel has obvious inhibitory effect on bladder tumor, and its inhibitory effect is much greater than that of free DOX. Therefore, this self-healing injectable hydrogel has great potential for *in situ* treatment of bladder cancer.

The injectable property of hydrogel has broadened its application as an implantable material in biological devices, minimally invasive treatment, and 3D biological scaffolds [1–4]. Injectable gels as drug delivery carrier play an active role in the field of local cancer treatment [5,6]. In clinical, local chemotherapy combined with 3D injection drug platform as an adjunct to surgical treatment is very effective in the treatment of non-metastatic tumors, especially bladder cancer which is prone to relapse after resection [7–11]. Chemotherapy for bladder cancer requires high doses and frequent infusions of drugs that cause a lot of physical pain and financial burden to patients, because the concentration of chemotherapy drugs decreases rapidly with the excretion of urine [12]. To improve the efficacy of drugs, the construction of bladder *in situ* hydrogel to treat bladder cancer has become a new therapeutic method [13]. Ding and Hou found that cationic polypeptide hydrogels had high adhesion and permeability in the bladder wall, and achieved good efficacy in the *in vivo* treatment of *in situ* bladder cancer in rats [14].

Chitosan (CS), as a medical absorbable natural cationic polymer, is a good carrier for cell culture and drug encapsulation [15,16]. Possessing many amino groups on the main chain, chitosan can be assembled with the anionic compounds *via* electrostatic interactions or cross-linked with boric acid, phosphate compounds, metal ions, and aldehyde derivatives [17–19]. Jiang and Shi jointly constructed a nanoparticle-hydrogel cascade reaction system with chitosan that could be infused into the bladder to induce apoptosis of tumor cells by increasing the accumulation of ammonia in cells [20]. The cascade reaction system is complex and prone to failure, so we hope to use cationic chitosan to construct a simple injectable gel system with high drug load for the *in situ* treatment of bladder cancer. Cyclodextrins (CDs) have broad application in drug loading and transportation, absorption-filtration and flexible electronic devices [21–23]. There have been many previous works showing that cyclodextrin supramolecular systems can significantly improve the bioavailability of anticancer drugs in active sites [24,25]. Nanoparticles of CS/SBE-β-CD for encapsulation of tea polyphenols, levofloxacin, and forearm bases have been reported [26–28]. Although the cavity of cyclodextrin can realize the solubilization of drugs, it is difficult to achieve 100% encapsulation of drugs in nanoparticle systems. The development of high-loading and targeted drug system is of great significance for chemotherapy treatment [29–31]. We can solve this problem by encapsulating the drug directly in the hydrogel in one step. Moreover, the properties of gels that are supportive and can change their shape at will are important for injectable gels. Sun *et al.* proposed a gel strategy in which ultrafast complexation between CS and Ag^+ was used to fabricate gels with high water content and shape indepen-

☆ This paper is dedicated to the memory of Prof. Jiang Wei.

* Corresponding authors.
E-mail addresses: yuqilin@mail.nankai.edu.cn (Q. Yu), chenyong@nankai.edu.cn (Y. Chen), yuliu@nankai.edu.cn (Y. Liu).

https://doi.org/10.1016/j.cclet.2023.108556
1001-8417/

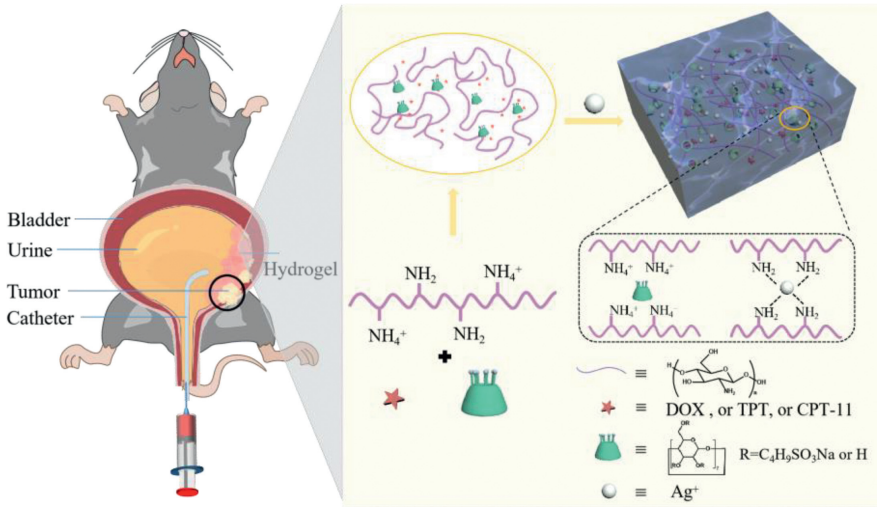

Scheme 1. The construction of supramolecular injectable CCA-DOX hydrogels for bladder cancer treatment.

dence [32]. However, the gelation has a concentration dependence on Ag^+, and the gel is too strong to be injected under the external force. Therefore, constructing a multi-component system where introducing chitosan, cyclodextrin, and silver ions to utilize multi-component composite effect and achieve suitable mechanical properties.

Here, by simple mixing chitosan, sulfobutyl ether-β-cyclodextrin (SBE-β-CD), Ag^+, we prepared the CS/SBE-β-CD/Ag^+ hydrogels (hereinafter referred to as CCA hydrogels). The electrostatic interaction between CS and SBE-β-CD and the dynamic covalent interaction between chitosan and silver ions cooperate to build the hydrogel network. The gel was injected through a syringe, and the obtained hydrogel filaments can heal into new gel clumps within 40 min. The results showed that the CCA hydrogels showed good self-healing properties, which made the hydrogel maintain a certain three-dimensional shape and suitable for human body elasticity after injection. Also by mixing chitosan, drug, SBE-β-CD, and silver ions, the drug was directly loaded into the hydrogel. The resulting hydrogel was named CCA-drug hydrogel. Most of the anticancer drugs can be effectively loaded into the 3D porous hydrogel networks. Furthermore, the affinity of cyclodextrins cavities for drugs enables cyclodextrins to carry some drugs. Considering the good biocompatibility of both CS and SBE-β-CD as well as the easy preparation, this hydrogel may be used as a convenient platform for minimally invasive local drug delivery. To evaluate the *in vivo* antitumor ability of the DOX-loaded gel CCA-DOX against *in situ* MB49-luc bladder tumors, we injected the gel into the bladder of mice. Ultimately, mice that received CCA-DOX showed very low levels of luciferase and a threefold higher survival rate compared to the free DOX group. Therefore, the CCA-DOX gel, which has demonstrated significant inhibition against bladder cancer tumors, has a high potential for use in intravesical chemotherapy.

Scheme 1 shows the construction process of dynamically self-healing and injectable hydrogel in which CS was cross-linked with SBE-β-CD and silver ion. Firstly, the pH value of chitosan solution (0.6 wt% in HAc) was changed to 5.5 with NaOH solution (0.1 mol/L), and then SBE-β-CD was mixed to the solution. Subsequently, a small amount of Ag^+ (0.06 mol/L) was added, and finally the hydrogel could be obtained within 30 s. The detailed steps of hydrogel preparation are presented in the supporting information. Herein, the electrostatic interaction between chitosan and SBE-β-CD as well as the complexation of Ag^+ with amino groups on the CS chain jointly lead to the formation of interlaced hydrogel networks. SEM images of CCA hydrogels (Figs. 1a and b) clearly

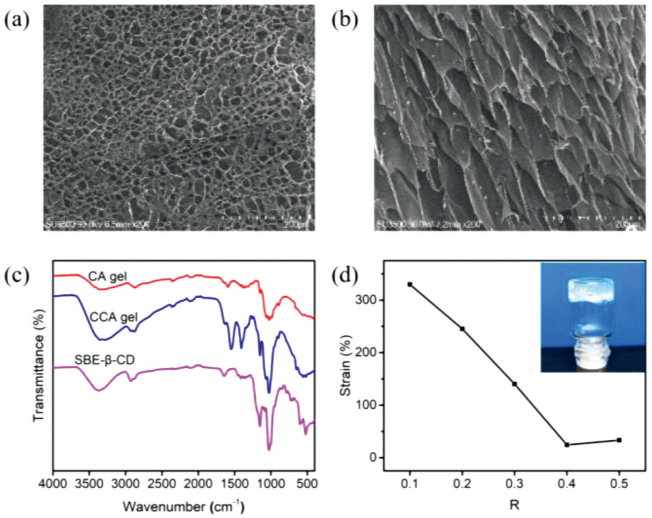

Fig. 1. SEM images of the CCA hydrogels after frozen drying. (a) surface; (b) cross-section. (c) FT-IR spectra of the CA xerogel, the CCA xerogel, and SBE-β-CD powders. (d) The strain value of the CCA hydrogels with different R values at the point of $G' = G''$, $R = m_{SCD}/m_{CS}$.

show its 3D porous network. The FT-IR spectra (Fig. 1c) of CCA xerogel showed several characteristic peaks assigned to ν_{OH} and ν_{NH} absorptions of CS (3347 cm^{-1} and 3285 cm^{-1}) [33] as well as $\nu_{S=O}$ absorptions [34] of SBE-β-CD (1630 cm^{-1}). Uniformly using 2 wt% chitosan solution, the CCA hydrogels with different concentrations of Ag^+ and SBE-β-CD were prepared. Table S1 (Supporting information) shows the coagulation conditions of various CA hydrogels and CCA hydrogels at different R values and Ag^+ concentrations by the reversed vial tests. For convenience, we defined $R = m_{SCD}/m_{CS}$. We found that when the concentration of Ag^+ decreased, the gelation times of CCA hydrogels greatly increased. Even with 0.015 mol/L Ag^+, gel time of CCA hydrogels is within 30 s.

To determine the effects of SBE-β-CD on the properties of CCA hydrogels and find the suitable condition for the construction of injectable hydrogels, we prepared a series of CCA hydrogels with different m_{SCD}/m_{CS} values ($R = 0.1$, 0.2, 0.3, 0.4, 0.5) at a fixed Ag^+ concentration (0.015 mol/L). Their rheological properties were measured. The strain amplitude sweep curves of CCA hydrogels ($R = 0.1$-0.5) with an angular frequency (1 Hz) and a strain range

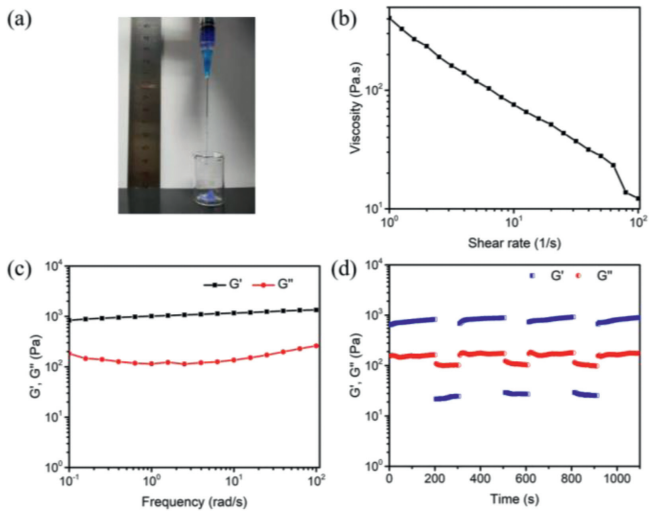

Fig. 2. (a) Injection experiments of the CCA-1 hydrogel with a 2 mL syringe. (b) The viscosity of the CCA-1 hydrogel with shear rates of 0.1 s^{-1} to 100 s^{-1} at 1% strain and 1 Hz angular frequency. (c) G' and G'' of the CCA-1 hydrogel at 1% fixed strain by frequency scanning (frequency = 0.1–500 rad/s). (d) G' and G'' of the CCA-1 hydrogel when the strain changed from low strain (1.0%) to high strain (1000%) at a 1 Hz angular frequency. The low strain was kept for 200 s, large strain was kept for 100 s.

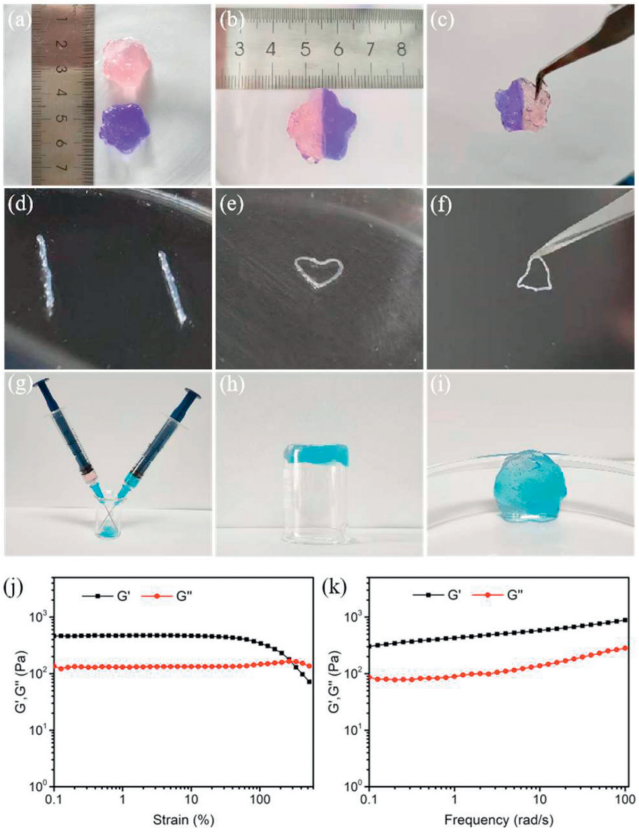

Fig. 3. Macroscopic self-healing experiments of CCA-1 hydrogels. (a) Two kinds of disk hydrogel (one was dyed with red dye, the other was dyed with purple dye). (b) The hydrogels were cut into 2 equal parts, and one of them was spliced together. (c) The spliced hydrogel plate can be suspended by tweezers and without splitting at 37 °C after healing for 1 h. (d) Two gel threads produced by 2 mL syringe dyed with blue dye. (e) Two gel threads were placed in the form of head to head and tail to tail connection. (f) The spliced hydrogel wires can be suspended by tweezers and without disconnecting at 37 °C after healing for 20 min. (g, h) The two hydrogels were dyed with red dye and blue dye respectively and injected into a 5 mL small beaker. (i) The self-healing hydrogel dish was set at 25 °C for 40 min. The above healing process occurred without any external intervention. (j) The strain sweep test (strain ranged 0.1% to 500% at 1 Hz) and (k) the frequency sweep test (frequency = 0.1-500 rad/s) at 1% strain of the fused self-healing hydrogel obtained from Fig. 3i.

of 0.1%∼500% at 37 °C were displayed in Fig. S1 (Supporting information). We found that the G' of all hydrogel samples was always greater than G'', indicating the good elasticity of these hydrogels. To some extent, the higher yield stress represents the larger stress required for the deformation of hydrogel, indicating that the hydrogel is difficult to be injected [19]. In other words, the lower modulus and the higher strain at the yield point correspond to the lower yield stress of the gel, which means the hydrogel is easy to be injected. Table S2 (Supporting information) shows the storage modulus and strain values of the CCA hydrogels ($R = 0.1–0.5$) at different yield points and gel points according to the strain amplitude sweep experiment results. From Table S2, it could be seen that among a series of hydrogels, the CCA-1 hydrogel has the maximum strain and the minimum modulus, indicating that this hydrogel is easily to be injected. In addition, as shown in Fig. 1d, the CCA-1 hydrogel has the highest strain at the gel point, indicating its good shaping ability. With suitable elastic modulus (∼1000 Pa) and viscosity (∼400 Pa s) [35], The CCA-1 gel is an excellent biomaterial for soft tissue (Figs. 2b and c). As the frequency varied from 0.1 rad/s to 100 rad/s, G' and G'' showed no obvious changes, indicating that the structure of the hydrogel relaxation is small as time goes on (Fig. 2c). The strain-step cyclic scanning is shown in Fig. 2d. Under the low strain of 1% for 200 s, the CCA-1 hydrogel remained gel state ($G' > G''$), subsequently changed to sol ($G' < G''$) at 1000% high strain for 100 s. After 4 cycles, the G' and G'' of the gel did not decrease, indicating that the gel had good recovery performance. Moreover, according to the mass ratio of lyophilized gel to initial hydrogel, the water content of the CCA-1 hydrogel is 93%. The hydrogel has good thermal stability that does not dehydrate after heating at 80 °C for 1 h (Fig. S2 in Supporting information). Therefore, the CCA-1 hydrogel was chosen as a model hydrogel for the in-depth study.

Injectable gels put more emphasis on low yield stress and self-healing properties. The self-healing properties of hydrogels were further evaluated by cutting-splicing. Two flower-type hydrogels stained separately with red dye and purple dye were cut apart (Figs. 3a and b). Then, half of the different colored hydrogels were combined into a mixed hydrogel plate. Without any external intervention, the boundary of hydrogels splicing section became blurred after 1 h at 37 °C. The fact that the flower-type hydrogel can be kept untracked by tweezers clamped on one side of the hydrogel (Fig. 3c) demonstrated the hydrogel had a good self-healing ability. The filamentary gels, as shown in Fig. 3d, were continuous and smooth, and they had good viscoelasticity and endured a slight stretch. In addition, two hydrogel lines produced by 2 mL syringes were healed in 20 min after the head to tail and tail to tail connection (Figs. 3d and e). Surprisingly, the accumulated hydrogel lines can quickly recover into a complete hydrogel plate after healing for 40 min (Figs. 3g-i). The two hydrogels were dyed with red dye and blue dye respectively and injected into a 5 mL small beaker (Fig. 3g), and inverting the beaker immediately, nothing flowed down. Stacks of hydrogel filaments were then kept undisturbed for 40 min in a small beaker at 37 °C to finally obtain discoidal hydrogels. Its surface was smooth and intact (Fig. 3i), accompanied by the good elasticity and stability measured by rheological tests (Figs. 3j and k).

We chose to load the three drugs DOX, CPT-11, and TPT into the CCA-1 gel, respectively. The procedure is to add Ag^{+} to a solution containing chitosan, drugs and SBE-β-CD, then shake well to get three CCA-drug gels. For either CA-DOX or CCA-DOX gels, the drug encapsulation rate was nearly 100%, the drug concentration

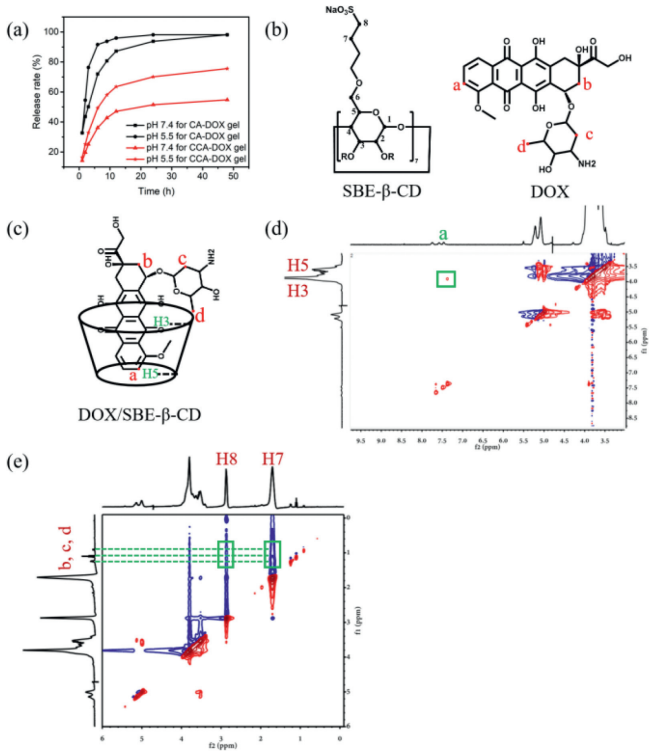

Fig. 4. (a) Time dependent release rate of CA-DOX hydrogels and CCA-DOX hydrogels in different pH release media (pH 5.5 and 7.2). (b) Structure of DOX and SBE-β-CD. (c) Structure of inclusion complex DOX/SBE-β-CD inferred from observed interactions. (d, e) Part of 2D NOESY (400 MHz, D_2O, 25 °C) spectra of inclusion complex of SBE-β-CD and DOX.

reached 300 μg/mL, and the drug loading rate was 0.03%. These three drugs had characteristic absorption at 478.5 nm, 367 nm, and 384 nm, respectively. Spectrophotometric standard curves for DOX, CPT-11, and TPT were obtained by measuring the three anticancer drugs characteristic absorptions (Fig. S3 in Supporting information). After the successful preparation of three drug-loaded gels CCA-DOX, CCA-CPT-11 and CCA-TPT, we performed the *in vitro* release test of drugs.

For CCA-DOX hydrogels, phosphate buffer (pH 7.2 and 5.5) was used to simulate the human *in vivo* environment and tumor microenvironment. By analyzing the drug concentration in buffer with time, the release ability of the gels for different drugs was observed. As shown in Fig. 4a, during the first 2 h, either the CA-DOX hydrogels or the CCA-DOX hydrogels experienced a rapid release of drug. The loaded drug in the CA-DOX hydrogels released nearly 57.5% within 2 h and totally released after 12 h. Compared with that of CA-DOX hydrogels, the release curves of CCA-DOX hydrogels were smoother. The drug release ratios of CCA-DOX hydrogels were 22% within the first 2 h and 78% in 48 h. In addition, the release ratios of CCA-DOX hydrogels at pH 5.5 were always larger than those at pH 7.4. On the other hand, the chemical structure of CPT-11 and TPT is lactone under acidic conditions, but it will change to carboxylate under physiological conditions (pH 7.4). Lactone ring is the necessary structure for irinotecan and topotecan hydrochloride to exert their antitumor activity, so the drug release experiment of CCA-CPT-11 and CCA-TPT hydrogels only need to be carried out at pH 5.5. From Figs. S4a and b (Supporting information), CCA-CPT-11 and CCA-TPT hydrogels both showed slow drug release. These jointly demonstrated the good control release ability of CCA-Drug hydrogels, especially in the tumor environment.

Compared with CA-DOX hydrogels, CCA-DOX hydrogels have better sustained release effect. We have made some speculations

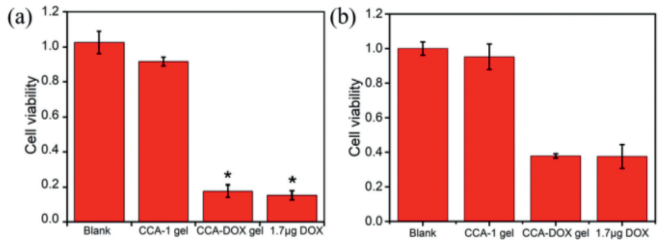

Fig. 5. Cytotoxicity experiments *in vitro* in 24 h ($n = 5$). Cellular viability of the MB49 bladder cancer cells (a), and the 293T human embryonic kidney cell lines (b) after treatment with blank (DMEM medium), CCA-1 hydrogels extract, and CCA-DOX hydrogels extract.

about the causes of these results. One possible reason may be that the electrostatic attraction between anionic cyclodextrin and cationic chitosan makes the three-dimensional network structure of hydrogels more compact, thus increasing the gel strength. Another reason is that the cavities of cyclodextrin also carry some drugs. The ^{1}H NMR spectra of SBE-β-CD, DOX and DOX/SBE-β-CD are shown in Fig. S5 (Supporting information). In the 2D NOESY spectrum in Fig. 4d, we can easily find the NOE cross peak between the Ha proton of DOX molecule and the H5 proton of SBE-β-CD molecule. This proves that DOX is contained in the SBE-β-CD cavity to form inclusion complexes. As can be seen from Fig. 4e, strong signals exist between the b, c and d protons of the glycoyl group on DOX and the H7 and H8 protons of SBE-β-CD, indicating the existence of electrostatic attraction between them, which also enables DOX to be loaded in the gel in large quantities.

Possessing the high encapsulation efficiency and the smooth control release property, the *in vitro* anticancer ability of CCA-DOX hydrogels was investigated by *in vitro* cytotoxicity experiments by using MB49 cells (a mouse bladder cancer cell line), HeLa cells (a cervical carcinoma cell line derived from Ms. Henrietta lacks) and 293T cells (derived from human embryonic kidney cells) as models. The CCA-1 hydrogels and CCA-DOX hydrogels were immersed in DMEM medium for 48 h to obtain hydrogel extracts. The concentration of free DOX was the same as the concentration of the DOX released from the hydrogels after 48 h. As shown in Fig. 5a, the viability of MB49 bladder tumor cells in the presence of CCA-DOX hydrogel was only 17%, which was very similar to that of free DOX (16%). Similar results were seen with HeLa cancer cells. The viability of HeLa cancer cells in the presence of CCA-DOX hydrogel was 7%, and the viability of free DOX was 6.5% (Fig. S6 in Supporting information). Using the culture medium containing CCA-1 hydrogels dip extracts, cells viability was 92% for MB49 cells and 94% for normal 293T cells after 24 h incubation (Fig. 5b). Therefore, these two results indicated that CCA-1 hydrogels as carriers had no obvious toxicity to normal cells and cancer cells, while CCA-DOX hydrogels had more obvious cytotoxicity to bladder cancer cells.

The *in vivo* antitumor capacity of the DOX-loading gels was further evaluated by using a MB49-luc cell-bearing bladder tumors, in which the MB49 tumor cells were labeled by luciferase to indicate the distribution of the tumor cells. *In vivo* imaging showed that while the mice received free DOX exhibited strong luciferase, the mice received the CCA-DOX gel exhibited extremely low intensity of luciferase (Figs. 6a and b). Moreover, 80% mice of the DOX group died on Day 12 (Fig. 6c), with the body weights remarkably decreased (Fig. 6d), indicating that free DOX was not efficient to inhibited the growth of the bladder tumor cells. In contrast, 80% mice of the CCA-DOX group survived even on Day 12, with the body weights were slowly recovered from Day 3. These results indicated that the CCA-DOX gel had much higher capacity than free DOX against the bladder tumors.

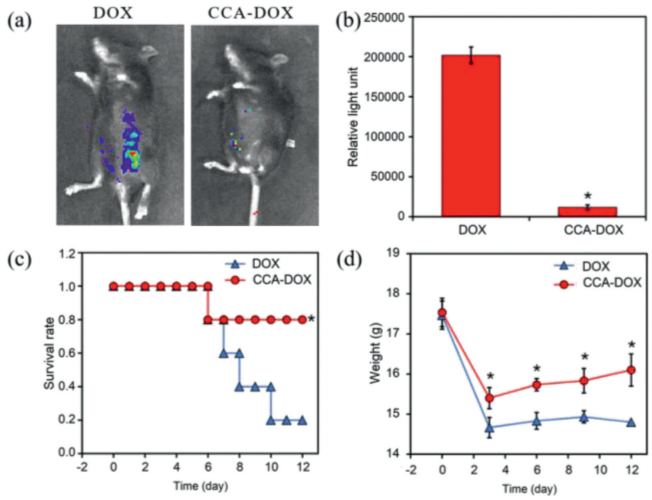

Fig. 6. *In vivo* antitumor capacity of free DOX and the DOX-loading gel CCA-DOX against the *in situ* MB49-luc-bearing bladder tumors. (a) Mouse imaging of the distribution of MB49-luc tumors after 6 days of treatment. The mouse bladders were firstly damaged by 0.1 mol/L HCl solution, followed by intravesical instillation of MB49-luc cells. After 5 days, the mice were intravesically injected by free DOX (5 mg/kg body weight) or CCA-DOX (containing 5 mg/kg DOX) one time per day on Day 0, 3, 6 and 9. On Day 6, the luciferase signals were detected by an *in vivo* animal imaging system. (b) Quantification of relative light unit of the mice. (c) Survival rate of the mice in each group. (d) Body weights of the mice in each group. The asterisks (*) indicated significant difference between the two groups ($P < 0.05$).

In conclusion, we successfully constructed a chitosan/SBE-β-CD supramolecular injectable hydrogel loaded with doxorubicin for the treatment of bladder cancer tumors. The gel heals quickly after injection and retains some human elasticity and stickiness. To evaluate the *in vivo* antitumor activity of DOX-loaded gel CCA-DOX against bladder tumors with MB49-luc *in situ*. The medicated gel was injected into the bladder of the mice. MB49 bladder cancer tumor cells were labeled with luciferase to indicate the distribution of tumor cells, and ultimately, mice that received CCA-DOX gel showed very low levels of luciferase and a threefold higher survival rate compared to the free DOX group. The CCA-DOX gel showed significant inhibitory effect on the growth of bladder tumor cells. Therefore, chitosan/SBE-β-CD loaded potion gel has great application potential in the treatment of bladder cancer.

Declaration of competing interest

The authors declare that they have no known competing financial interests or personal relationships that could have appeared to influence the work reported in this paper.

Acknowledgments

We thank National Natural Science Foundation of China (Nos. 22131008 and 21971127) and the Haihe Laboratory of Sustainable Chemical Transformations for financial support.

Supplementary materials

Supplementary material associated with this article can be found, in the online version, at doi:10.1016/j.cclet.2023.108556.

References

[1] L. Cheng, Z. Cai, T. Ye, et al., Adv. Funct. Mater. 30 (2020) 2001196.
[2] J. Bian, F. Cai, H. Chen, et al., Nano Lett. 21 (2021) 2690–2698.
[3] Y. Zhao, Z. Cui, B. Liu, et al., Adv. Healthcare Mater. 8 (2019) 1900709.
[4] Z. Wang, Y. Zhang, Y. Yin, et al., Adv. Mater. 34 (2021) 2108300.
[5] Y. Tu, N. Chen, C. Li, et al., Acta Biomater. 90 (2019) 1–20.
[6] J. Guo, R. Shen, X. Shen, et al., Chin. Chem. Lett. 33 (2022) 979–982.
[7] G.R. Shin, H.E. Kim, J.H. Kim, S. Choi, M.S. Kim, Pharmaceutics 13 (2021) 1953.
[8] F. Papaccio, S. Roselló, M. Huerta, et al., Cancers (Basel) 12 (2020) 3611.
[9] K. Zhang, L. Zhou, F. Chen, Y. Chen, X. Luo, J. Control. Release 315 (2019) 197–205.
[10] K.W. Luo, X. Zhu, T. Zhao, et al., Front. Cell Dev. Biol. 8 (2020) 606123.
[11] J. Zhang, Y. Guo, G. Pan, et al., ACS Appl. Mater. Interfaces 12 (2020) 21441–21449.
[12] P. Guo, L. Wang, W. Shang, et al., ACS Appl. Mater. Interfaces 12 (2020) 54367–54377.
[13] S. Shawky, S. Makled, A. Awaad, N. Boraie, Pharmaceutics 14 (2022) 2527.
[14] H. Guo, F. Li, W. Xu, et al., Adv. Sci. 5 (2018) 1800004.
[15] G. He, X. Yan, Z. Miao, et al., Chin. Chem. Lett. 31 (2020) 1807–1811.
[16] S. Cheng, M. Pan, D. Hu, et al., Chin. Chem. Lett. 34 (2023) 108276.
[17] K.C. Cheng, C.F. Huang, Y. Wei, S.H. Hsu, NPG Asia Mater. 11 (2019) 25.
[18] M. Abrami, C. Siviello, G. Grassi, D. Larobina, Carbohydr. Polym. 214 (2019) 110–116.
[19] S. Ahmad, I. Khan, J. Pandit, et al., Int. J. Biol. Macromol. 221 (2022) 435–445.
[20] W. Jing, C. Chen, G. Wang, et al., Adv. Sci. 10 (2023) 2206893.
[21] W. Xu, Y. Chen, B. Zhang, et al., Biomacromolecules 22 (2021) 4434–4445.
[22] Y.H. Zhang, Y. Chen, Chin. Chem. Lett. 34 (2023) 107836.
[23] S.S. Jia, W.S. Xu, Y. Chen, Y. Liu, Chin. Chem. Lett. 32 (2021) 2773–2776.
[24] L. Chen, Y. Chen, Y. Zhang, Y. Liu, Angew. Chem. Int. Ed. 60 (2021) 7654–7658.
[25] N. Li, Y. Chen, Y.M. Zhang, et al., Sci. Rep. 4 (2014) 4164.
[26] J. Wang, L. Feng, Q. Yu, Y. Chen, Y. Liu, Biomacromolecules 22 (2021) 534–539.
[27] X.M. Chen, Y. Chen, X.F. Hou, et al., ACS Appl. Mater. Interfaces 10 (2018) 24987–24992.
[28] F. Liu, J. Antoniou, Y. Li, et al., Food Hydrocoll. 57 (2018) 291–300.
[29] X.Y. Hu, L. Gao, S. Mosel, et al., Small 14 (2018) 18039.
[30] X. Tian, M. Zuo, P. Niu, et al., ACS Appl. Mater. Interfaces (13) (2021) 37466–37474.
[31] P. Zhang, X. Liu, W. Hu, Y. Bai, L. Zhang, Carbohydr. Polym. 149 (2016) 224–230.
[32] Z. Sun, F. Lv, L. Cao, et al., Angew. Chem. Int. Ed. 127 (2015) 8055–8059.
[33] R. Wang, Y. Tian, J. Wang, et al., Adv. Funct. Mater. 31 (2021) 2104488.
[34] X. Mao, R. Cheng, H. Zhang, et al., Adv. Sci. 6 (2019) 1801555.
[35] O. Chaudhuri, J. Cooper-White, P.A. Janmey, D.J. Mooney, V.B. Shenoy, Nature 584 (2020) 535–546.